

# Lawrence Berkeley National Laboratory

## Recent Work

### Title

LANTHANUM DIFFUSION IN MOLTEN URANIUM.

### Permalink

<https://escholarship.org/uc/item/4628p3dc>

### Author

Borgne, Edmond. Le

### Publication Date

1969-10-01

UCRL-19072

*cy. J*

RECEIVED  
LAWRENCE  
RADIATION LABORATORY

DEC 5 1969

LIBRARY AND  
DOCUMENTS SECTION

LANTHANUM DIFFUSION IN MOLTEN URANIUM

Edmond Le Borgne  
(M. S. Thesis)

October 1969

AEC Contract No. W-7405-eng-48

TWO-WEEK LOAN COPY

This is a Library Circulating Copy  
which may be borrowed for two weeks.  
For a personal retention copy, call  
Tech. Info. Division, Ext. 5545

LAWRENCE RADIATION LABORATORY  
UNIVERSITY of CALIFORNIA BERKELEY

UCRL-19072

*cy. J*

## **DISCLAIMER**

This document was prepared as an account of work sponsored by the United States Government. While this document is believed to contain correct information, neither the United States Government nor any agency thereof, nor the Regents of the University of California, nor any of their employees, makes any warranty, express or implied, or assumes any legal responsibility for the accuracy, completeness, or usefulness of any information, apparatus, product, or process disclosed, or represents that its use would not infringe privately owned rights. Reference herein to any specific commercial product, process, or service by its trade name, trademark, manufacturer, or otherwise, does not necessarily constitute or imply its endorsement, recommendation, or favoring by the United States Government or any agency thereof, or the Regents of the University of California. The views and opinions of authors expressed herein do not necessarily state or reflect those of the United States Government or any agency thereof or the Regents of the University of California.

## LANTHANUM DIFFUSION IN MOLTEN URANIUM

Edmond Le Borgne

Inorganic Materials Research Division, Lawrence Radiation Laboratory,  
Department of Nuclear Engineering, College of Engineering,  
University of California, Berkeley, California

### ABSTRACT

The purpose of this study was to measure the diffusion coefficient of lanthanum in molten uranium, at microscopic and macroscopic concentrations.

In order to get the diffusing element at microscopic concentrations, a uranium rod was irradiated to generate approximately  $10^{-9}$  atom fraction lanthanum 140. The irradiated rod was placed next to an unirradiated rod and the lanthanum allowed to diffuse into the unirradiated uranium rod. The diffusion of lanthanum was determined by measuring the intensity of the 1.6 MeV lanthanum 140 photopeak along the rod. However, the diffusion process at such low concentrations could not be represented by a diffusion coefficient and could not be separated from mixing due to convection and to melting and freezing.

The diffusion coefficient of lanthanum in molten uranium at macroscopic concentrations ( $\sim 0.01$  atom fraction lanthanum) was measured by putting a small amount of lanthanum on top of a uranium rod, letting it diffuse, and measuring the penetration of lanthanum along the rod. The diffusion coefficient obtained by this method,  $\sim 4 \times 10^{-7} \text{ cm}^2 \text{ sec}^{-1}$ , was much lower than expected. The reason for the low diffusivities was probably the presence of bubbles or voids in the liquid uranium.

## INTRODUCTION

Studies of solute diffusion in liquid metals contribute to the understanding of the liquid state. The diffusion of fission products in molten uranium is also of interest for the pyrometallurgical method of reprocessing nuclear fuels, since the diffusion of these elements to a phase boundary is the first step in the extraction mechanism.<sup>1</sup>

Many diffusion coefficients in liquid metals have already been measured, and their order of magnitude is usually  $10^{-5}$  cm<sup>2</sup> sec<sup>-1</sup> or greater.<sup>2</sup> A study of the diffusion of lanthanum in molten uranium has not yet been reported, although Smith<sup>3</sup> has measured the diffusivity of cerium in uranium.

Diffusion coefficients in liquid metals are measured by essentially three techniques.<sup>4</sup> The capillary reservoir technique is the most popular. In this method, a small tube containing pure solvent metal is inserted in an alloy bath. After having been kept at a certain temperature for a definite time, during which diffusion proceeds, the small tube is drawn up, quenched and analyzed. In the second technique, a small tube is filled with pure solvent up to about half of its height, then filled up compactly with alloy and suspended in a tube which is kept in an electric furnace. The third method was used by Kitchener and coworkers.<sup>5</sup> The pure solvent metal is fused in vacuum and a small glass tube is filled up to about half of its height with this metal. After a small amount of alloy is placed on the solvent metal, the tube is sealed off in vacuum, and

the remaining procedures are the same as in the second method. The experimental procedure used here was inspired by the third method.

## I. LANTHANUM DIFFUSION IN MOLTEN URANIUM AT TRACER CONCENTRATIONS

### A. Experimental Procedure and Apparatus

A cylindrical piece of depleted uranium metal (0.2% uranium 235) 2 in. long and 1/8 in. diameter (weight = 7.5 gms) was irradiated inside an evacuated quartz ampoule for 8 hours and cooled for one week. The atom fraction of lanthanum 140 produced by fission was then  $\sim 10^{-9}$ .

The sample was removed from its capsule inside a glove box flushed with argon. The irradiated piece and another identical unirradiated piece were inserted in a beryllia crucible, which was in turn inserted into a molybdenum container. The assembly was then loaded into a pyrex container, evacuated by a diffusion pump, and transferred to the LRL machine shop for electron beam welding of the top lid on the molybdenum can. The electron beam welding was done under vacuum so that the metals were exposed to air only during the time required to load into the welder. The completed assembly, shown in Fig. 1, was leak tested, then suspended inside the hot zone of a vacuum resistance furnace as shown in Fig. 2. The furnace was evacuated to approximately  $5 \times 10^{-4}$  torr. Power was then applied to the furnace to raise the temperature above the melting point of uranium. The temperature was kept constant during the amount of time desired for the diffusion. At the end of this period, the furnace was turned off and the sample solidified. When the assembly was cool enough, it was removed from the furnace for counting.

The penetration of lanthanum into the unirradiated uranium rod was determined by measuring the intensity of the 1.6 MeV lanthanum 140 photopeak along the length of the uranium rod. This nuclide, however, is not produced directly by uranium fission but is the daughter of barium 140 which is produced with a direct yield of 6.4%. The decay chain is

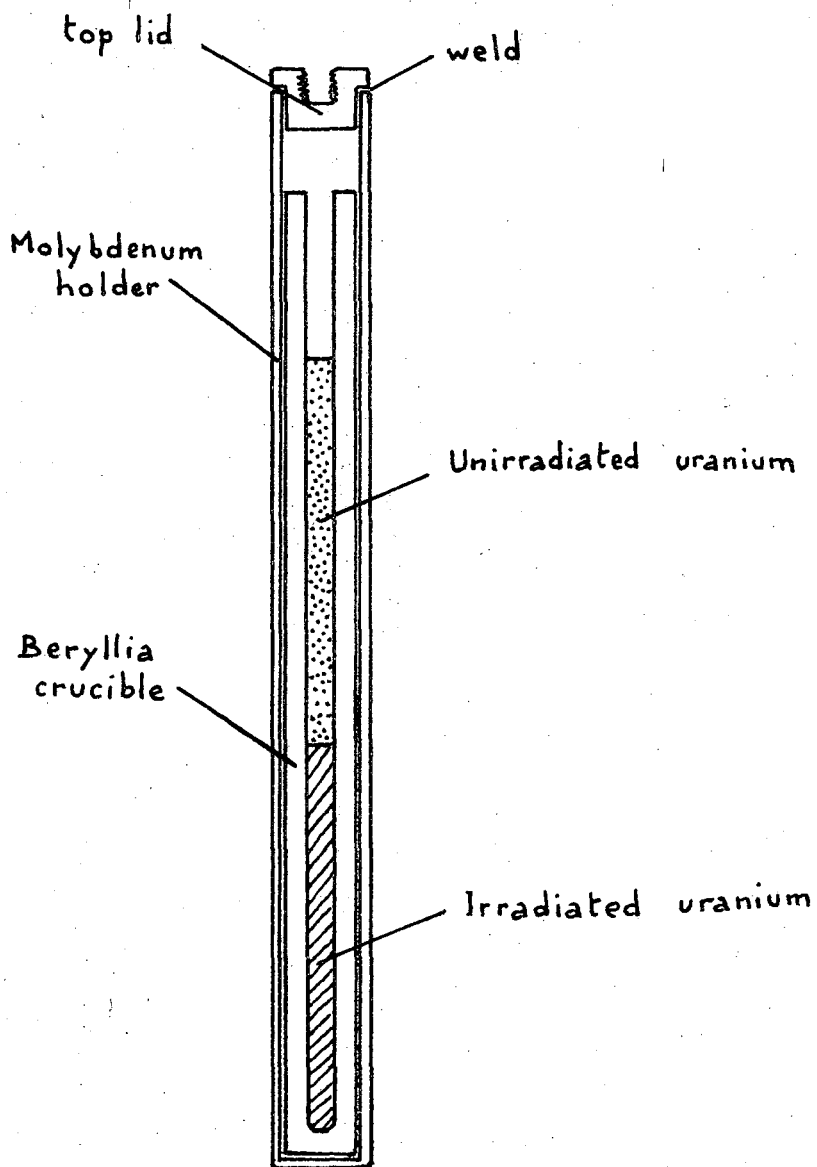


Fig. 1 Diffusion cell for tracer lanthanum diffusion studies.



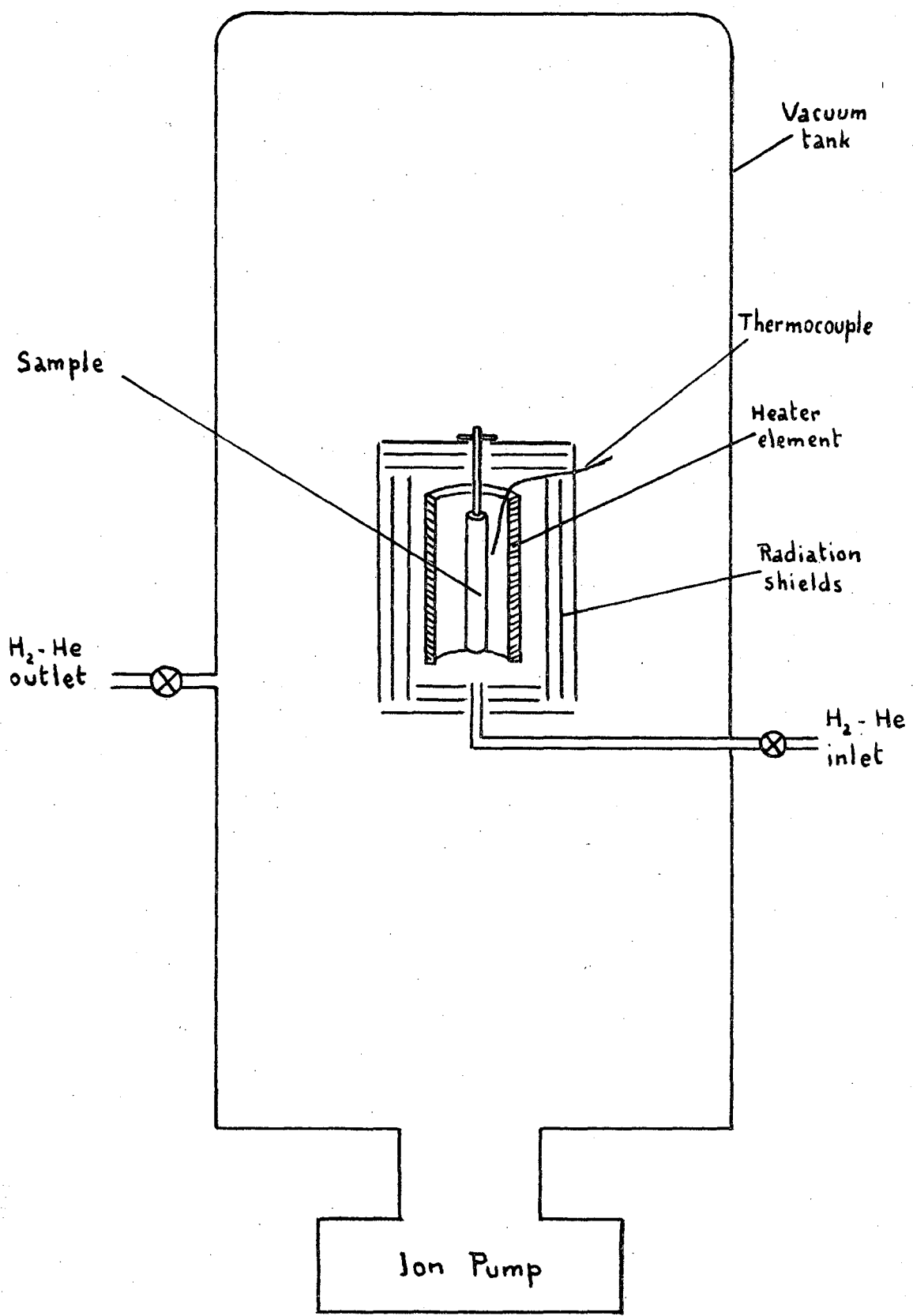
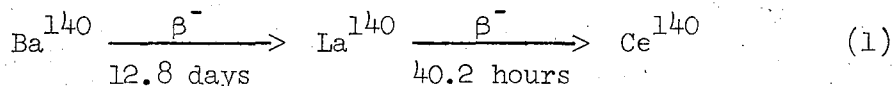


Fig. 2 Vacuum resistance furnace.



The radioactive nuclides, produced in the fission of uranium, which emit high-energy gamma rays tend to have short half-lives. Because of the long half life of its parent, however, the 1.6 MeV photon from lanthanum 140 decay dominates the gamma-ray spectrum of uranium which has been cooled for several days. The intensity of this photopeak served as a measure of the lanthanum-140 concentration in the uranium rod.

The detecting equipment is shown in Fig. 3. The size of the collimator in the lead shield is such that the detector views a 3 mm-thick slice of the uranium rod. The rod is moved up and down inside the lead shield by a screw whose displacement can be measured with a precision of 0.2 mm.

### B. Theoretical Analysis

1. The model of diffusion in a solid bounded by two parallel planes has been used. With an initial lanthanum concentration (or activity)  $a_{\text{La}}^i(x)$  and both ends  $x=0$  and  $x=l$  insulated (zero flux), the concentration profile  $a_{\text{La}}^o(x)$  immediately after a diffusion time  $\Theta$  is given by<sup>6</sup>

$$a_{\text{La}}^o(x) = \frac{1}{l} \int_0^l a_{\text{La}}^i(x') dx' + \frac{2}{l} \sum_{n=1}^{\infty} e^{-Dn^2\pi^2\Theta/l} \cos \frac{n\pi x}{l} \int_0^l a_{\text{La}}^i(x') \cos \frac{n\pi x'}{l} dx' \quad (2)$$

In terms of the dimensionless parameters

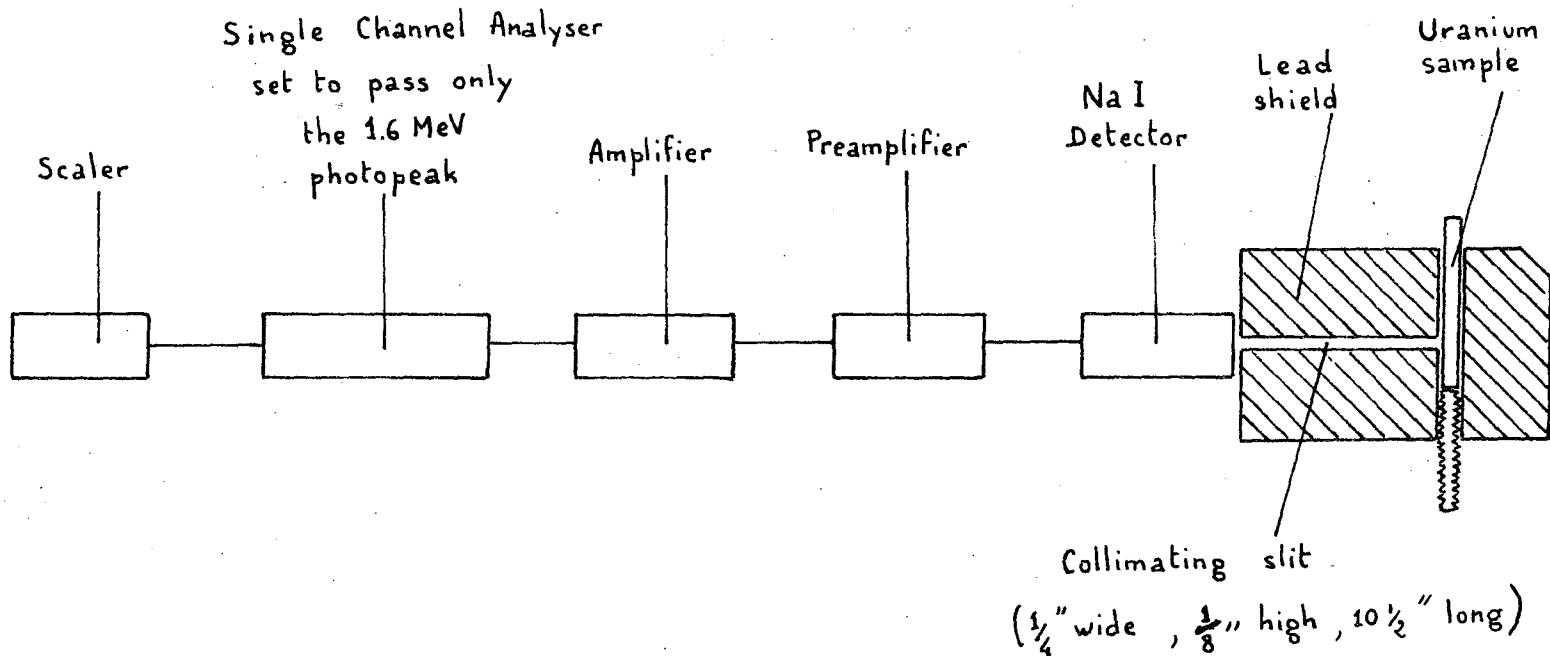


Fig. 3 Block diagram of the counting equipment.

$$\tau = \frac{D_0}{l^2} \quad (3)$$

$$\eta = \frac{x}{l} \quad (4)$$

this can be written

$$a_{La}^o(\eta) = \int_0^1 a_{La}^i(\eta') d\eta' + 2 \sum_{n=1}^{\infty} e^{-n^2 \pi^2 \tau} \cos n\pi\eta \int_0^1 a_{La}^i(\eta') \cos n\pi\eta' d\eta' \quad (5)$$

Calling

$$A_n = 2 \int_0^1 a_{La}^i(\eta') \cos n\pi\eta' d\eta' \quad (6)$$

the Fourier coefficients of the initial concentration profile  $a_{La}^i(x)$ , the profile after diffusion is thus

$$a_{La}^o(\eta) = \frac{A_0}{2} + \sum_{n=1}^{\infty} A_n \cos n\pi\eta e^{-n^2 \pi^2 \tau} \quad (7)$$

This series is rapidly converging. However, the first fifty terms were taken into account to determine the curves corresponding to different values of the diffusion coefficient. The initial activity profile  $a_{La}^i(x)$  was measured and used to determine the  $A_n$  of Eq. (6). The theoretical curves were compared to the experimental curves to determine the diffusion coefficient (or value of  $\tau$ ) which best fitted the data.

## 2. Determination of the Lanthanum Concentration Profile Immediately After Diffusion

The decay scheme of Eq. (1) leads to a lanthanum activity at any position in the uranium rod given as a function of time by the well known relation for batch decay of a two-member chain

$$\frac{a_{La}}{a_{La}^0} = \frac{e^{-\lambda_{Ba}t}}{F} + \left(1 - \frac{1}{F}\right) e^{-\lambda_{La}t} \quad (8)$$

where  $t$  is the time after the diffusion experiment and the parameter  $F$  depends upon the initial ratio of the two nuclides at  $t=0$

$$F = \frac{N_{La}^0}{N_{Ba}^0} \frac{\lambda_{La} - \lambda_{Ba}}{\lambda_{Ba}} \quad (9)$$

This gives

$$a_{La} e^{\lambda_{Ba}t} = \frac{a_{La}^0}{F} + a_{La}^0 \left(1 - \frac{1}{F}\right) e^{(\lambda_{Ba} - \lambda_{La})t} \quad (10)$$

The lanthanum concentration profile was measured at different times  $t$  after diffusion.  $a_{La} e^{\lambda_{Ba}t}$  was plotted versus  $e^{(\lambda_{Ba} - \lambda_{La})t}$ , giving a straight line whose slope was  $a_{La}^0 \left(1 - \frac{1}{F}\right)$  and intercept was  $a_{La}^0/F$ . This permitted determination of the lanthanum concentration profile immediately after diffusion,  $a_{La}^0$ , at all positions within the rod.

### C. Results

1. The purpose of the first run was to determine the mixing due to melting and freezing the two uranium rods (with no diffusion time), and to represent this mixing by an equivalent value of  $(D\theta)$ , or an equivalent dimensionless parameter  $\tau^*$ .

The sample was held at 1200°C for approximately 2 minutes and cooled down immediately. This operation was repeated three times, and the resulting concentration profiles are shown as curves 2, 3 and 4 in Fig. 4, (the points have been corrected for lanthanum decay after the experiment).

The determinations of  $\tau^*$  for these premelts were made starting with

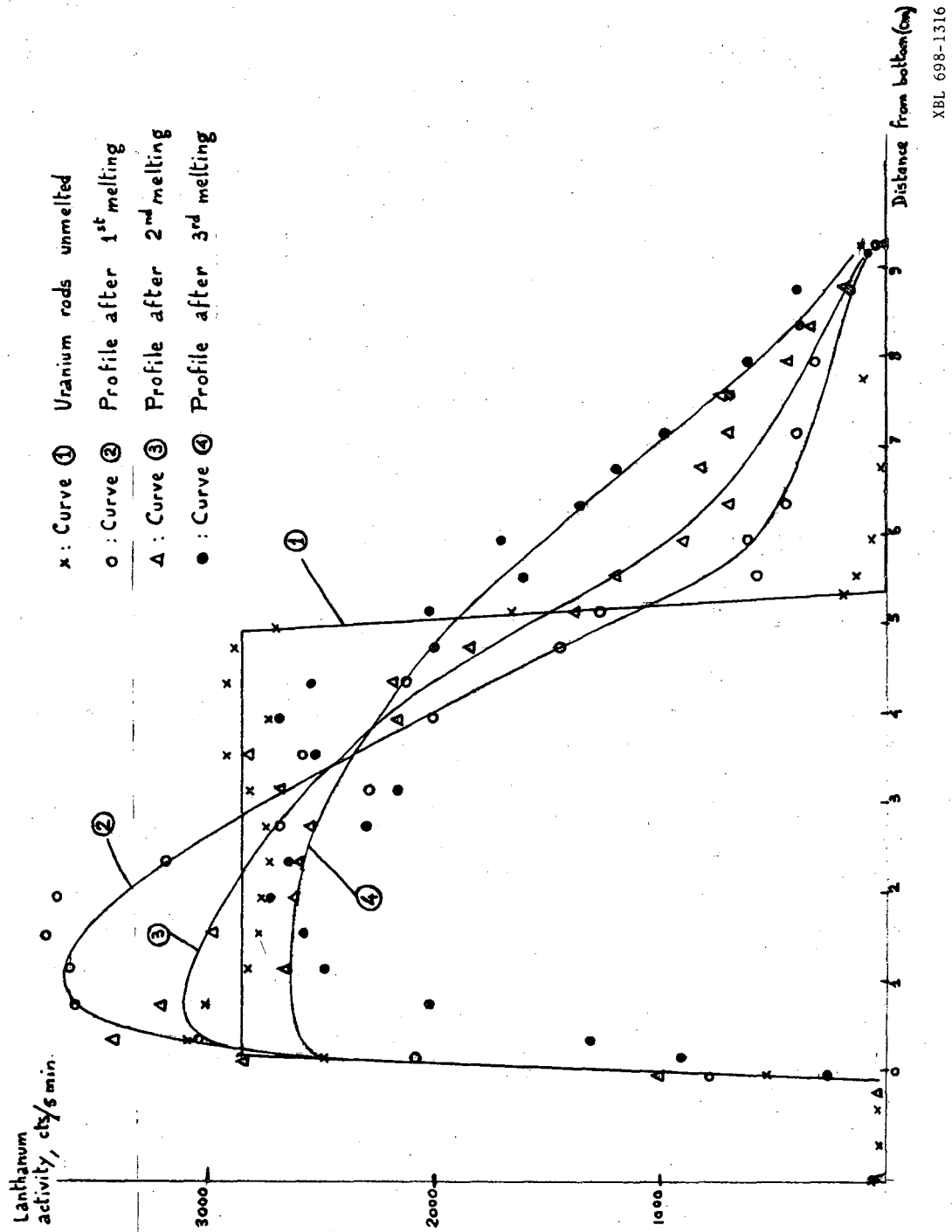


Fig. 4 Successive premelts of two uranium rods.

a curve corresponding to uranium rods already melted, since before the first melting the uranium rods were not yet in their final position (some slumping occurs during melting of the machined rods, which are somewhat smaller in diameter than the inner diameter of the crucible).

The results of the first premelt (concentration profile changing from curve 2 to curve 3), as shown in Fig. 5, are best fitted by a theoretical diffusion curve corresponding to a value of  $\tau^*$  of 0.015. In a typical diffusion run of 30 minutes, this would correspond to an equivalent diffusion coefficient of  $7 \times 10^{-4} \text{ cm}^2 \text{ sec}^{-1}$ .

The second premelt (concentration profile changing from curve 3 to curve 4), as shown in Fig. 6, was much more difficult to represent by a diffusion curve. The equivalent  $\tau^*$  would have been still larger than in the first determination, lying between 0.015 and 0.025.

## 2. Diffusion Experiment

The two uranium rods (one of them irradiated) were first melted for 2 minutes and cooled, so that they were in their final position before performing the diffusion experiment. The sample was removed from the furnace and the lanthanum concentration profile was measured. The sample was reinserted in the furnace and held at  $1240^\circ\text{C}$  for 30 minutes. The concentration profile was measured at different times after the diffusion run, and the lanthanum profile immediately after diffusion was determined following the method described in Section B-2.

The results of the diffusion experiment are shown in Fig. 7. Here again, the measured penetration was considerably different from the theoretical penetration due to a pure diffusional process. The value of  $\tau$  representing the actual data could not be determined with a satisfactory precision, but was probably between 0.02 and 0.04.

Fig. 5 First premelt.

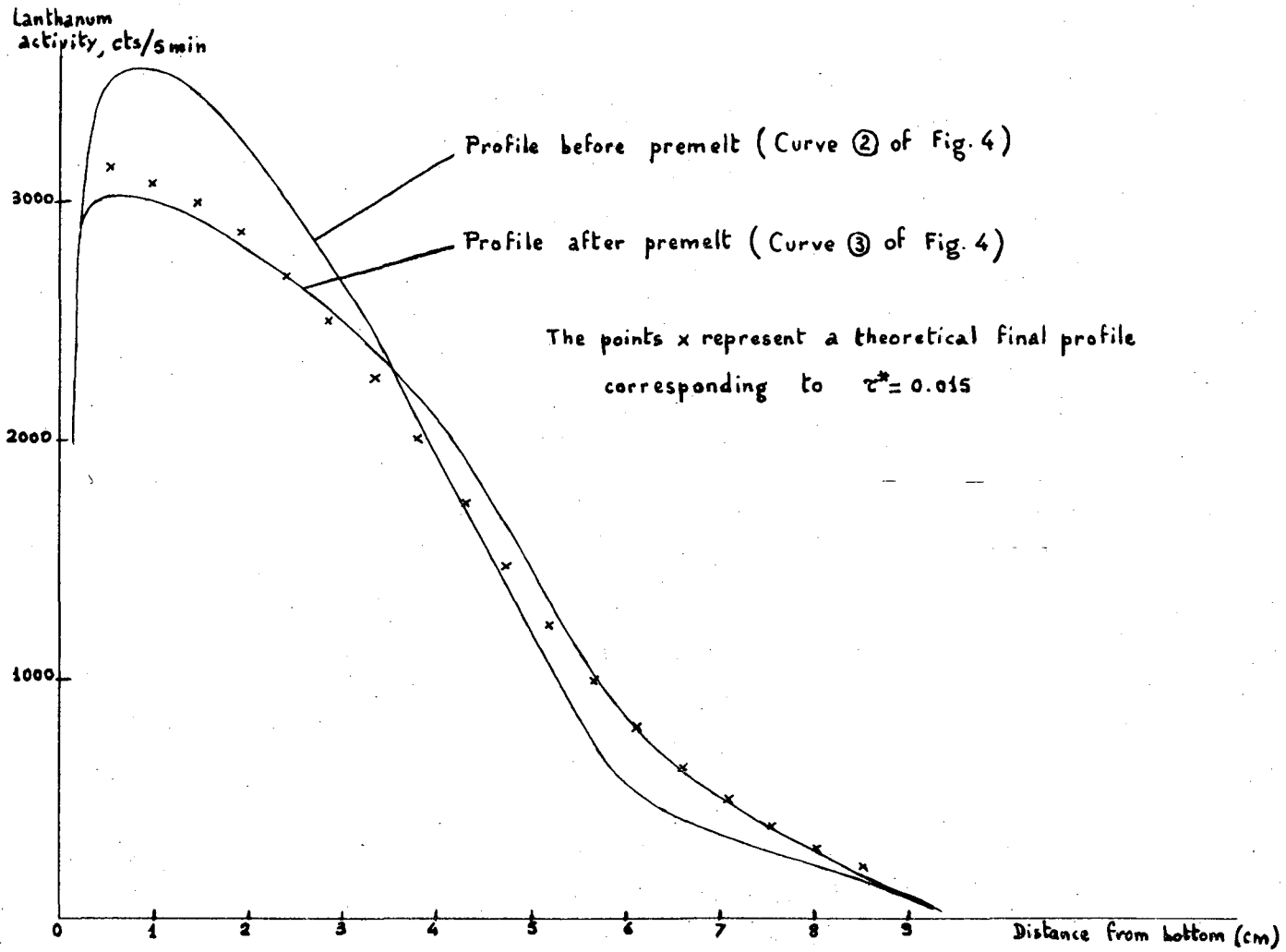




Fig. 6 Second premelt.

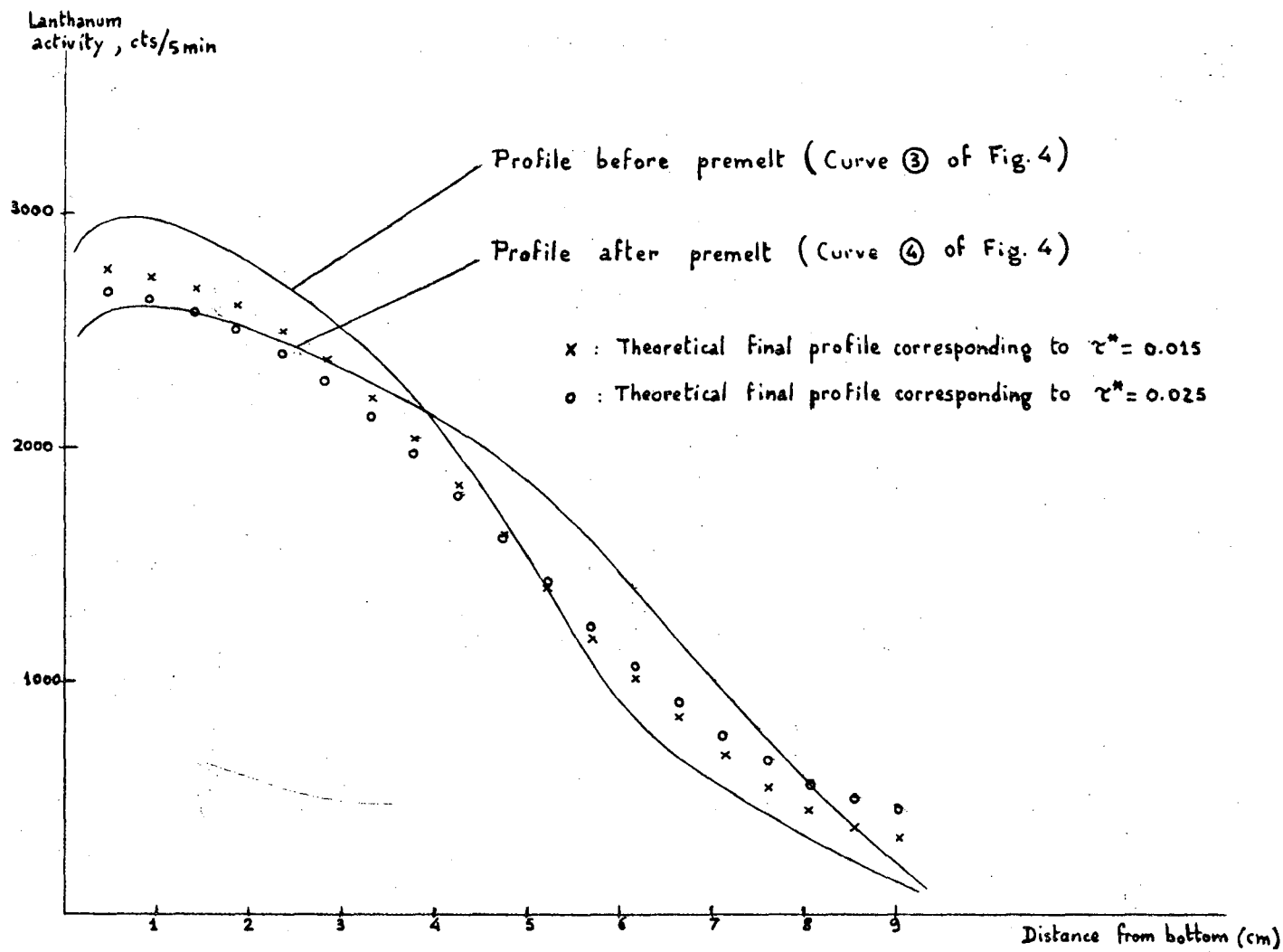
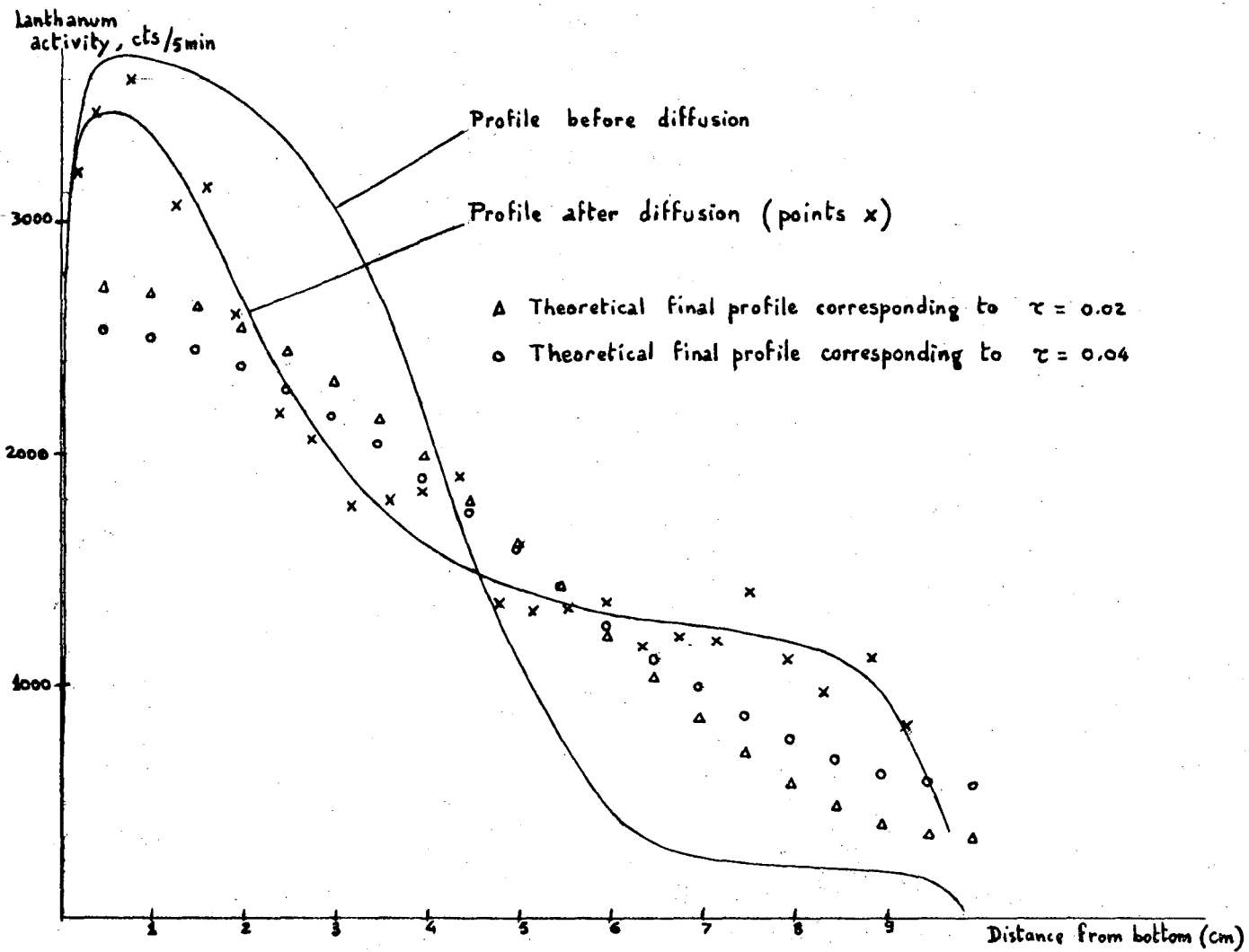


Fig. 7 Diffusion experiment.



Since the total  $\tau$  measured is the sum of  $\tau^*$  due to melting and freezing the sample, and  $\tau_d = \frac{D\theta}{l^2}$  due to diffusion,

$$\tau = \tau^* + \tau_d$$

the mixing due to diffusion itself is less than the mixing due to melting and freezing the sample. Since the latter could not be represented with a good approximation by an equivalent diffusion coefficient, the uncertainty on the value of  $\tau_d$  was unacceptable.

#### D. Conclusion

Interdiffusion of fission product lanthanum between an irradiated and an unirradiated uranium rod did not permit determination of the diffusion coefficient of lanthanum in molten uranium. The mixing due to diffusion was small compared to external causes of mixing, among which the major one seemed to be convection. A study of the temperature distribution in the furnace showed that the top of the hot zone was colder than the bottom by more than 70°C. Furthermore, the experimental points in the determination of the lanthanum concentration profile were far from being on a smooth curve, which suggested that defects like bubbles could be present in the uranium rods used. Avoiding those two sources of error was the main object in the study of lanthanum diffusion in molten uranium at macroscopic concentrations discussed in Part II. Moreover, the very small concentration of lanthanum 140 in the uranium ( $10^{-9}$  atom fraction) was very easily scavenged by oxygen impurities in the uranium. Since  $\text{La}_2\text{O}_3$  is thermodynamically more stable than  $\text{UO}_2$ , even 1 ppm of oxygen in the uranium would have been sufficient to convert all lanthanum metal to lanthanum oxide. The use of macroscopic lanthanum concentrations avoids this scavenging problem.

## II. LANTHANUM DIFFUSION IN MOLTEN URANIUM AT MACROSCOPIC CONCENTRATIONS

### A. Experimental Procedure and Apparatus

The experimental method and apparatus were basically the same as in Part I. Two kinds of crucibles were used to hold the uranium and lanthanum liquids. The first type was the same as the beryllia crucible with molybdenum holder shown in Fig. 1. In this kind of crucible, one unirradiated uranium rod was inserted. The second crucible was tantalum in which two unirradiated uranium rods could be inserted. The uranium rods were the same as those used in the study of lanthanum diffusion at tracer concentrations.

After the uranium was inserted in the crucible, the crucible (with no top lid) was placed in the vacuum resistance furnace of Fig. 2. The furnace was evacuated to approximately  $10^{-6}$  torr. The temperature was then kept at  $1000^{\circ}\text{C}$  during 10 hours for outgassing before melting the uranium. The temperature was then set to  $1300^{\circ}\text{C}$  and kept constant for 3 hours. During the melting of the uranium, the pressure while above the melting point ( $1132^{\circ}\text{C}$ ) never exceeded  $4 \times 10^{-6}$  torr. The sample was then cooled down and kept under vacuum until the lanthanum was ready to be inserted into the crucible.

The lanthanum used was 99.9% pure metal kept under dry nitrogen atmosphere. A cylindrical piece of 0.1 in. diameter and 0.5 in. long (weight = 0.5 gm) was scraped until the metal was shiny (a thin white oxide layer develops on the surface of the metal after a few minutes exposure to air), wiped off and loaded into a polyethylene snap-top irradiation capsule. These operations were performed in a glove box flushed with dry nitrogen. The sample was then irradiated for 30 minutes to generate approximately 20 mCi of lanthanum  $^{140}$  by neutron capture in La-139 (> 99% natural abundance.) The irradiated lanthanum was placed on

top of the uranium in the glove box and the crucible capped and placed in a glass vial. The vial was removed from the glove box and evacuated, then transported to the LRL machine shop where the crucible was sealed by electron beam welding (also under vacuum) and leak tested.

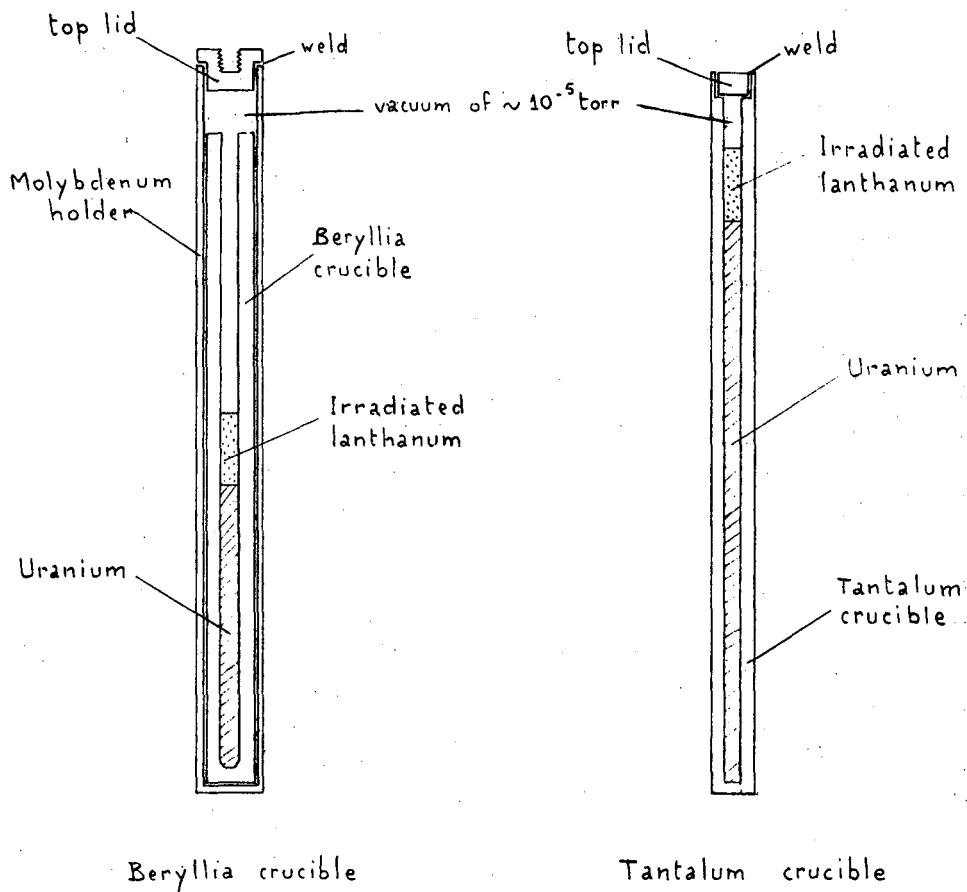
The completed assembly, shown in Fig. 8 was then inserted in the furnace and melted. In order to minimize convection, the furnace was flushed with helium-hydrogen (4%) at a flow rate of 8 cubic feet per hour so that the bottom of the crucible was colder than the top by 10°C. The temperature was kept constant during the time desired for the diffusion experiment. The sample was then cooled down and removed from the furnace for counting. As in Part I, the penetration of lanthanum into uranium was determined by measuring the intensity of the 1.6 MeV lanthanum-140 photopeak along the assembly. The counting equipment was the same as in Part I and is shown in Fig. 3.

#### B. Theoretical Analysis

The model of diffusion in a semi-infinite medium has been used, since the lanthanum penetration never reached the end of the uranium rod. With a lanthanum concentration (or activity)  $C_0$  maintained at the equilibrium solubility at  $x=0$  (interface) and no lanthanum initially in the region  $x > 0$ , the lanthanum concentration after a diffusion time  $\theta$  is given as a function of the distance  $x$  from the interface by

$$\frac{C}{C_0} = 1 - \operatorname{erf} \frac{x}{2\sqrt{D\theta}} = \operatorname{erfc} \frac{x}{2\sqrt{D\theta}} \quad (11)$$

where  $\operatorname{erfc}$  is the complementary error function. Plots of the inverse complementary error function of  $C/C_0$ ,  $\operatorname{erfc}^{-1}(C/C_0)$ , versus  $x$  gives straight lines passing through the origin with slope  $\frac{1}{2\sqrt{D\theta}}$ .



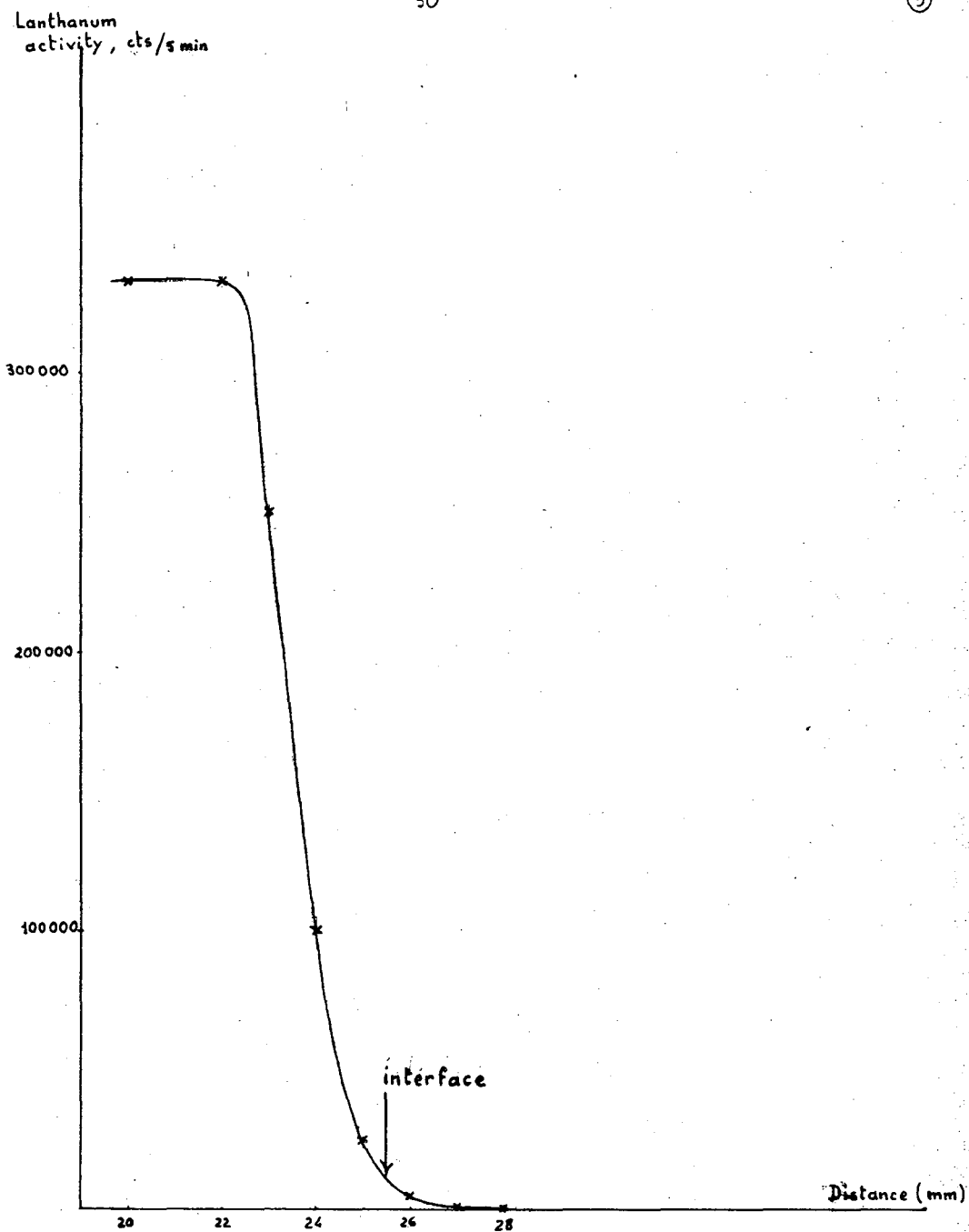
XBL 698-1327

Fig. 8 Diffusion cells for bulk concentration lanthanum diffusion experiments.

The main problem was the location of the position of the interface between lanthanum and uranium in the lanthanum concentration profile after diffusion. The method chosen was to start from the low concentration end of the profile, which resembled a diffusion curve. The region where the curve departed significantly from an error function curve was taken as the interface. This procedure was verified by determining the solubility of lanthanum in uranium by comparing the lanthanum-140 activity at the chosen interface position to that in the pure lanthanum rod above the interface. This calculation is discussed in detail in the subsequent section devoted to analysis of Run No. 3.

### C. Results

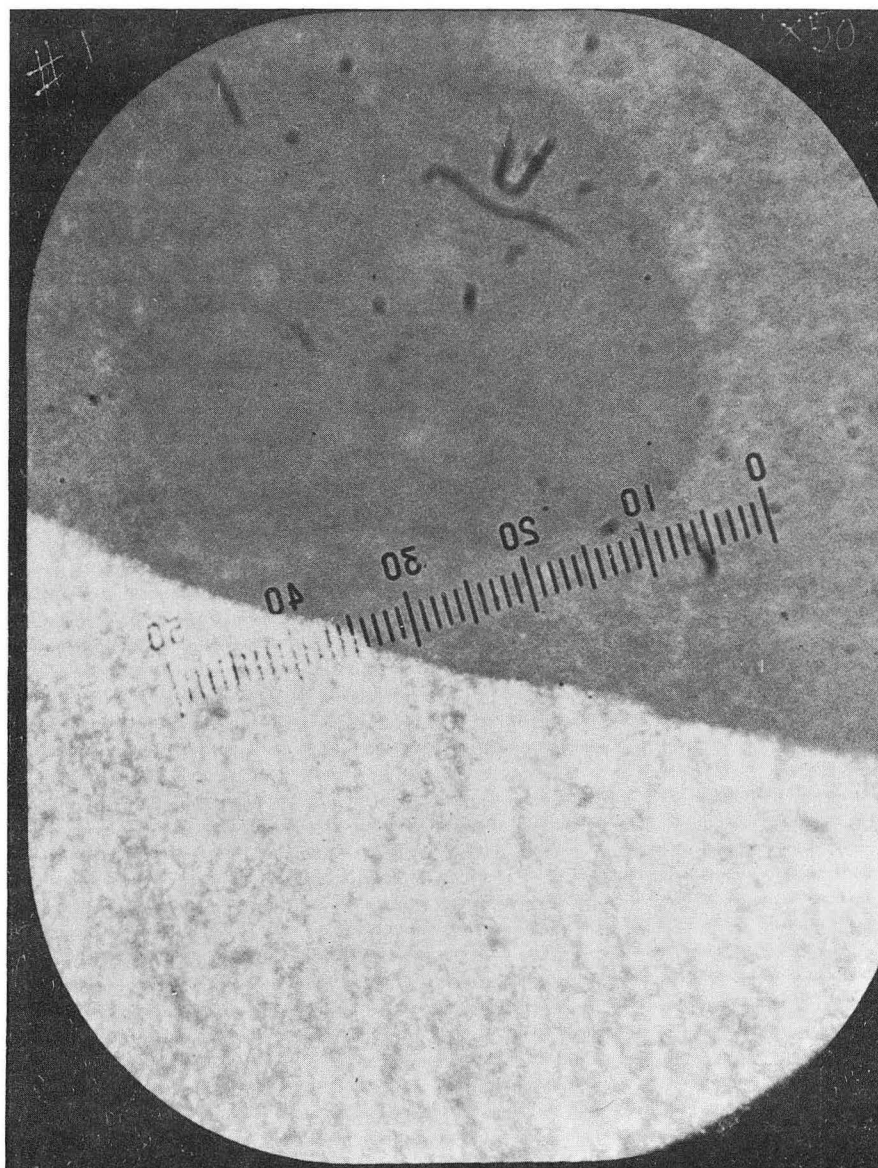
1. As in Part I, the purpose of the first run was to determine the amount of mixing due to melting and freezing the sample, with no diffusion time. The crucible used was a tantalum crucible. The sample was held at 1200°C for 2 minutes and cooled down immediately. The lanthanum concentration profile after melting is shown in Fig. 9. Two months after the experiment, when lanthanum-140 had almost completely decayed, the crucible was sawed lengthwise and polished, and pictures of the interface were taken. Figure 10 (×50 magnification) shows that the contact between the two metals was very good, even though a bubble was present in lanthanum approximately 1mm from the interface, as can be seen in Fig. 11 (×8.5 magnification). Figure 11 also shows that the meniscus at the interface was approximately 2 mm high. Looking at the profile shown in Fig. 9, it could thus be concluded that the penetration of lanthanum into uranium was less than 2.5 mm and could thus be neglected, a typical penetration in the diffusion runs being greater than 1 cm.



XBL 698-1320

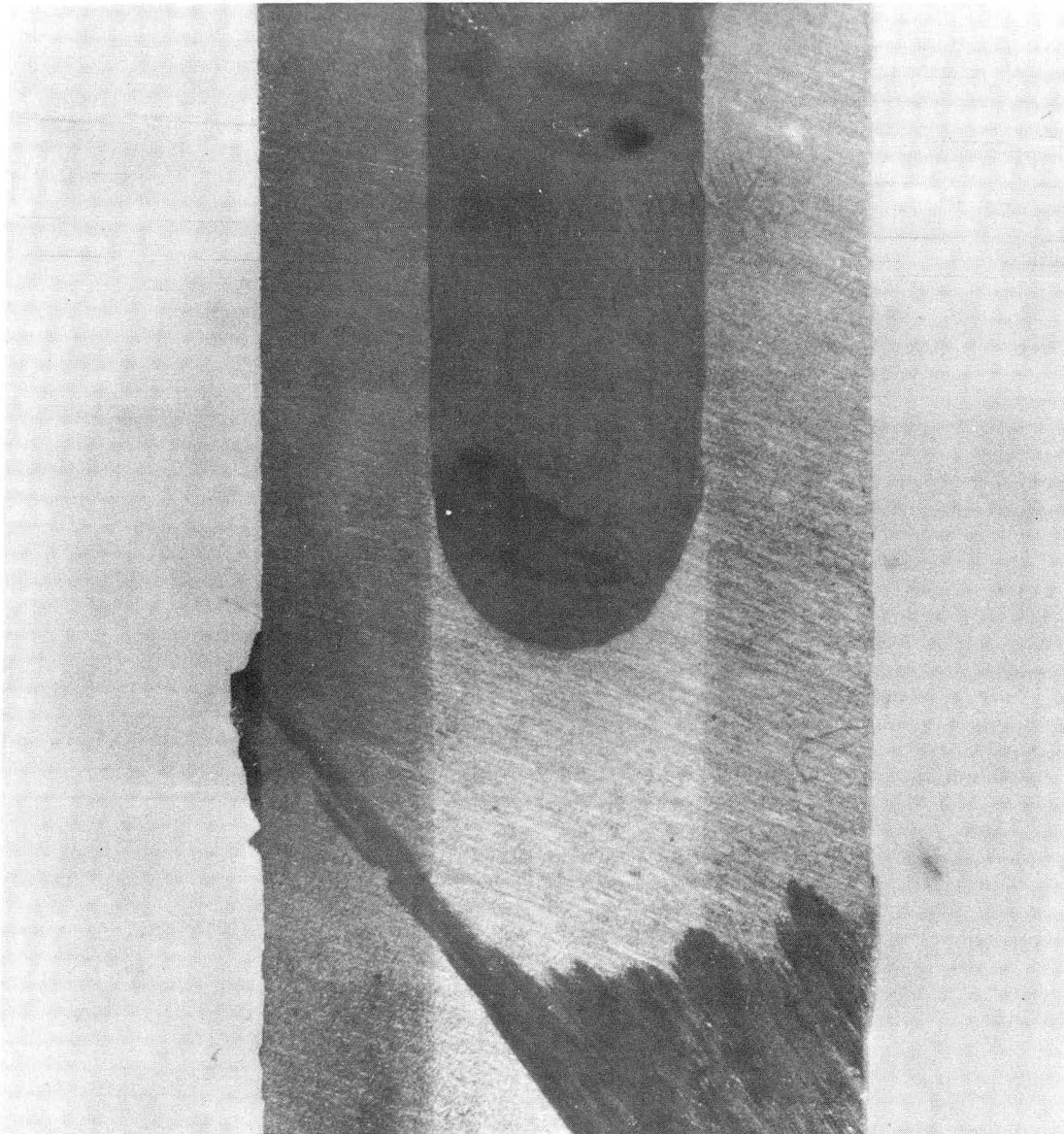
Fig. 9 Lanthanum concentration profile - Run no. 1.





XBB 698-5519

Fig. 10 Lanthanum-uranium interface -  
Run no. 1 ( $\times 50$  - Lanthanum on top).

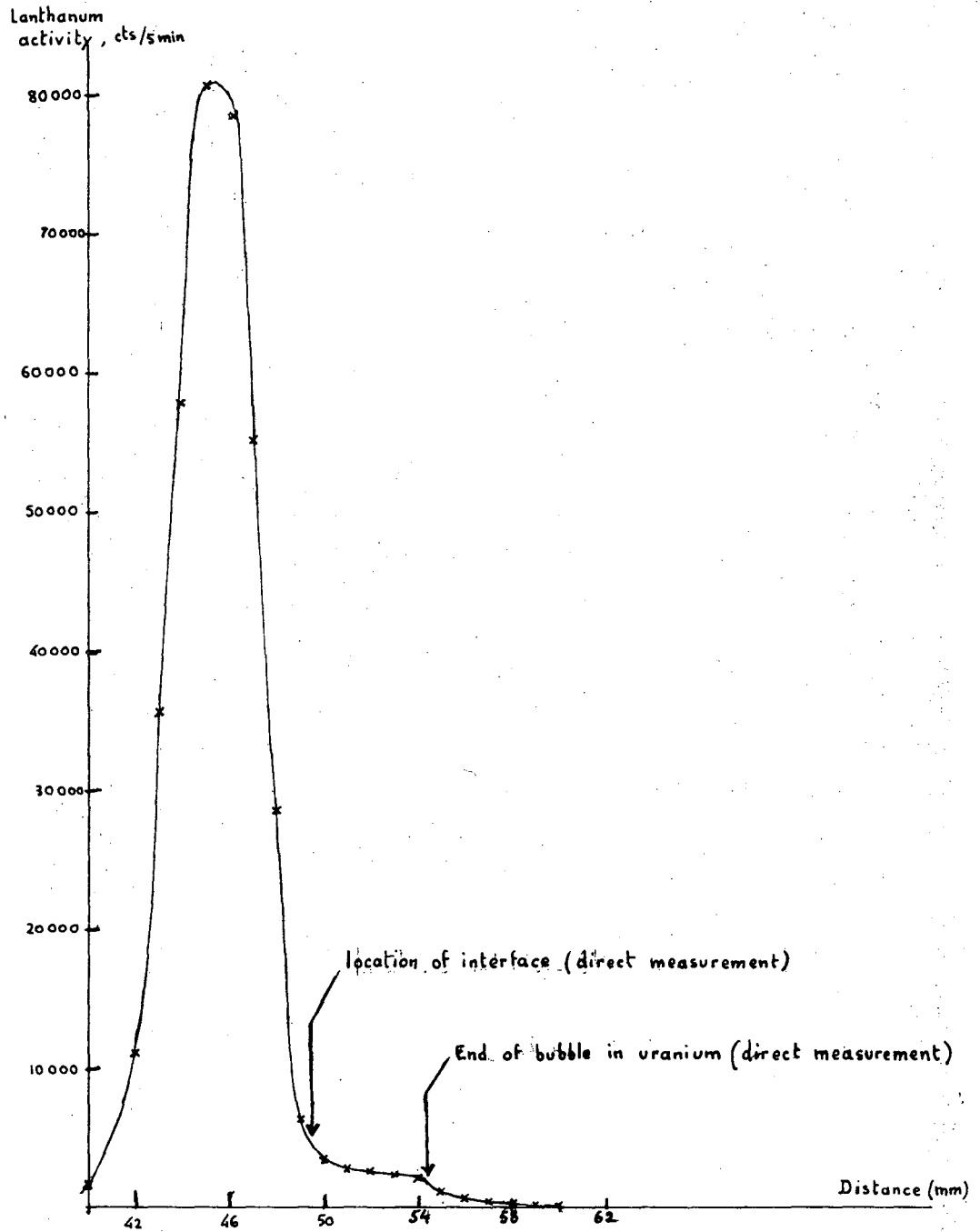


XBB 698-5518

Fig. 11 Lanthanum-uranium interface - Run no. 1  
( $\times 8.5$  - Lanthanum on top).

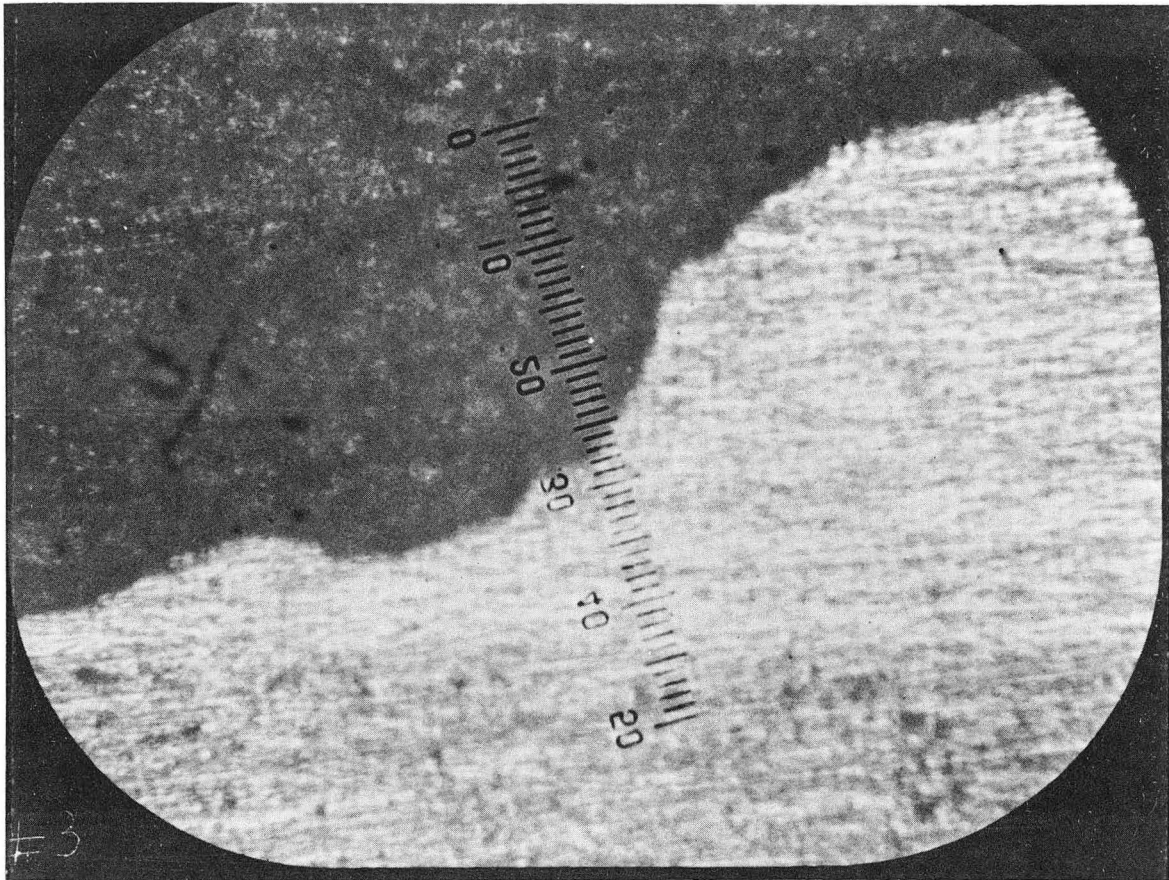
## 2. Diffusion Experiment in Tantalum Crucible (Run No. 3)

The first diffusion experiment was performed using a tantalum crucible. The sample was held at 1200°C for 24 hours and cooled down. The lanthanum concentration profile after diffusion is shown in Fig. 12. The determination of the interface was made easier when the sample could be sawed lengthwise 6 weeks after the experiment. Figure 13 gives a picture of the interface (x50 magnification) showing that the contact between the two metals was excellent even after 24 hours diffusion time. A general picture of the interface is shown in Figs. 14 and 15 (x8.5 magnification). There was a large bubble (3mm long) in the uranium, approximately 2mm from the interface, which can be seen on both Figs. 14 and 15. Comparing Fig. 14 to the lanthanum concentration profile shown in Fig. 12, the position of the lanthanum-uranium interface (bottom of the meniscus) could be located at position 49.5 in Fig. 12. However, the bubble must have blocked the penetration of lanthanum and kept a constant concentration at the extremity of the bubble (position 54.4 in Fig. 12). This extremity was thus acting like a second interface, and the region between  $x=50$  to  $x=54$  appeared to be lanthanum-saturated uranium. The maximum measured activity in the lanthanum part of the rod was ~80,000 count/.5 min. However, since the lanthanum occupied only a ~3mm height in the tantalum crucible (see Fig. 14), and the width of the window in the collimator was also 3mm, it is probable that neither of the two measurements around the maximum of Fig. 12 viewed pure lanthanum metal. Had the 3mm segment of lanthanum filled the entire collimator window, the activity would have been larger than 80,000, say ~100,000. The activity at the  $x=54$ mm position (which represents uranium saturated with lanthanum) was ~1700. The ratio  $1700/100,000 = 0.017$  atom fraction should be the solubility of lanthanum



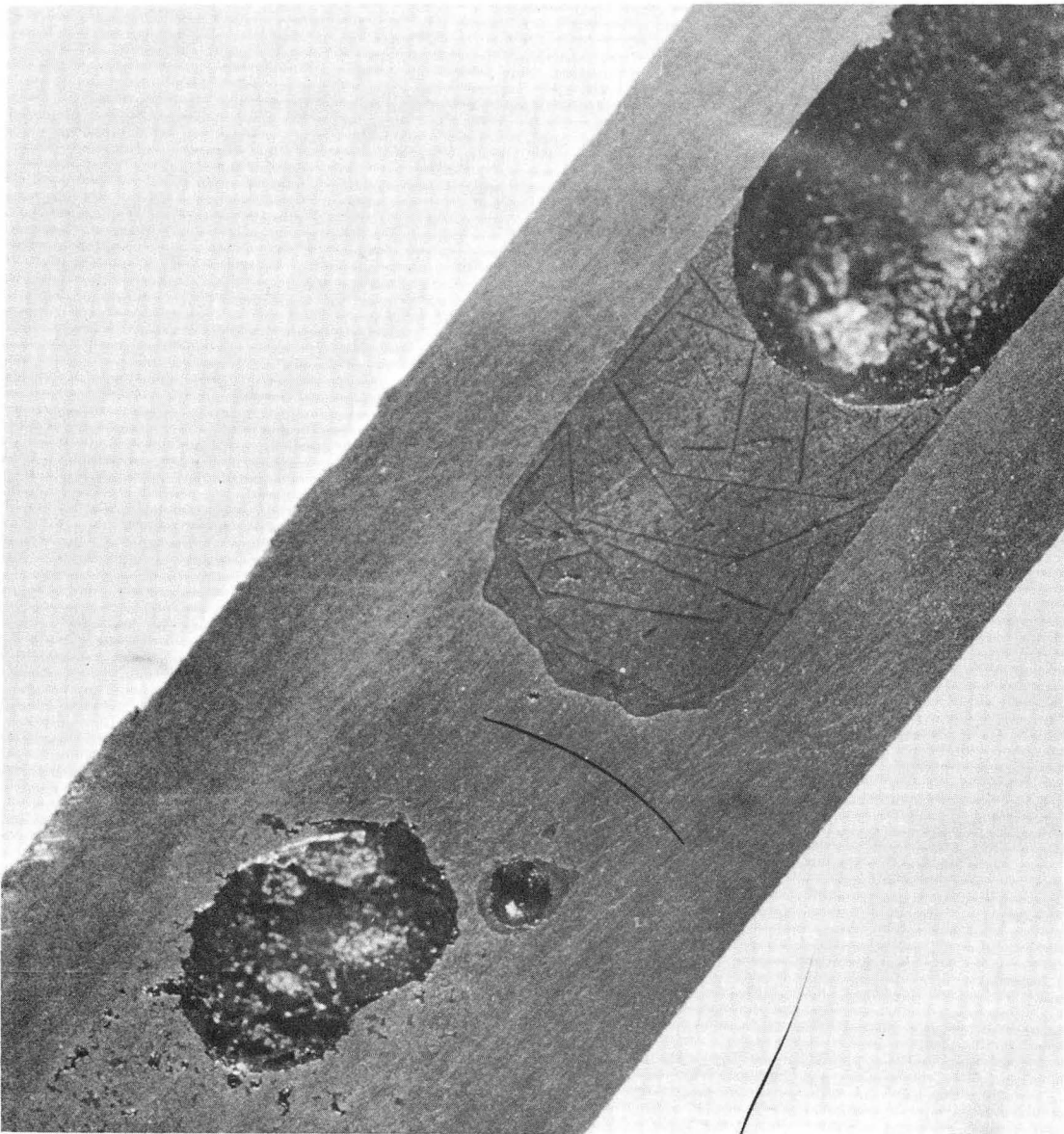
XBL 698-1321

Fig. 12 Lanthanum concentration profile after diffusion -  
Run no. 3.



XBB 698-5521

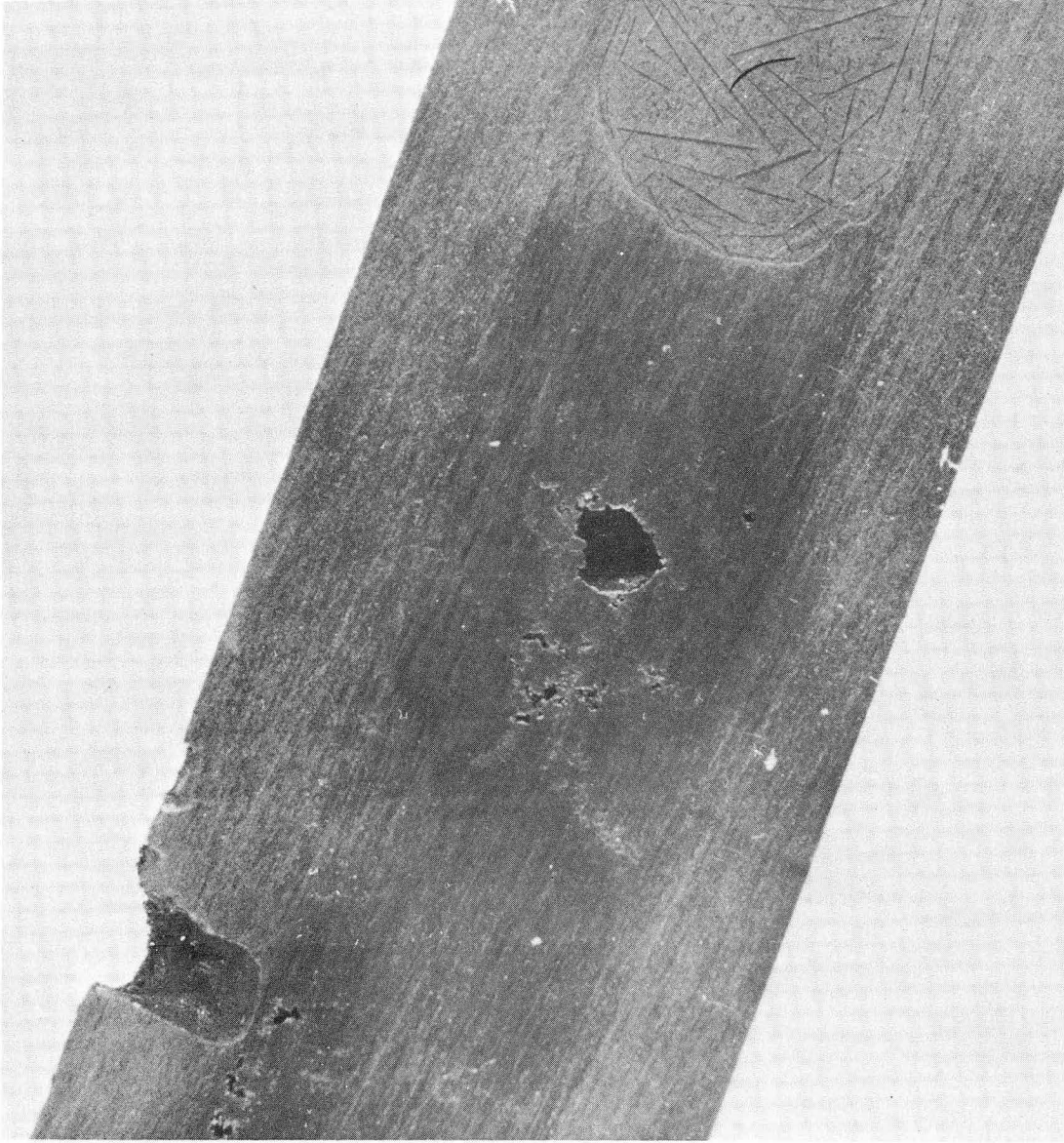
Fig. 13 Lanthanum-uranium interface - Run no. 3.  
(x50 - Lanthanum on top).



XBB 698-5517

Fig. 14 Left side of lanthanum-uranium interface -  
Run no. 3 ( $\times 8.5$  - Lanthanum on top).





XBB 698-5516

Fig. 15 Right side of lanthanum-uranium interface -  
Run no. 3 ( $\times 8.5$  - Lanthanum on top).

in uranium. This value is in reasonably good agreement with the solubility of 0.018 atom fraction measured by Haefling and Daane.<sup>7</sup>

Assuming that the activity at  $x = 54.4$  represented the saturation solubility of lanthanum in uranium, the penetration curve was determined with the "interface" located at this position. The ratio of the lanthanum concentration  $C$  to the lanthanum concentration at the interface  $C_0$  is plotted versus the distance  $x$  from the "interface" in Fig. 16. In Fig. 17 the inverse complementary error function of  $\frac{C}{C_0}$  is plotted versus  $x$ . The points are located with a very good approximation on a straight line passing through the origin. The slope of this straight line gave a value of  $4 \times 10^{-7} \text{ cm}^2 \text{ sec}^{-1}$  for the diffusion coefficient at  $1200^\circ\text{C}$ .

### 3. Diffusion Experiment in Beryllia Crucible (Run #5)

In order to check the reproducibility of the result obtained for the diffusion coefficient in Run #3, a second diffusion experiment was performed, the tantalum crucible being replaced by a beryllia crucible. The sample was held at  $1210^\circ\text{C}$  for 25 hours and cooled down. The lanthanum concentration profile after diffusion is shown in Fig. 18. In a picture of the interface ( $\times 50$  magnification) shown in Fig. 19, the contact between the two metals did not look as good as in the tantalum crucible. But this was probably due to the fact that the beryllia crucible had to be broken to take the picture, and it was then much more difficult to get a very smooth surface by polishing the rod, lanthanum being much softer than uranium. A general picture of the interface ( $\times 8.5$  magnification), shown in Fig. 20, did not reveal any large bubble in uranium near the interface, which was assumed to be located at position 67 in Fig. 18. Note that the curvature of the interface is in the opposite sense as in



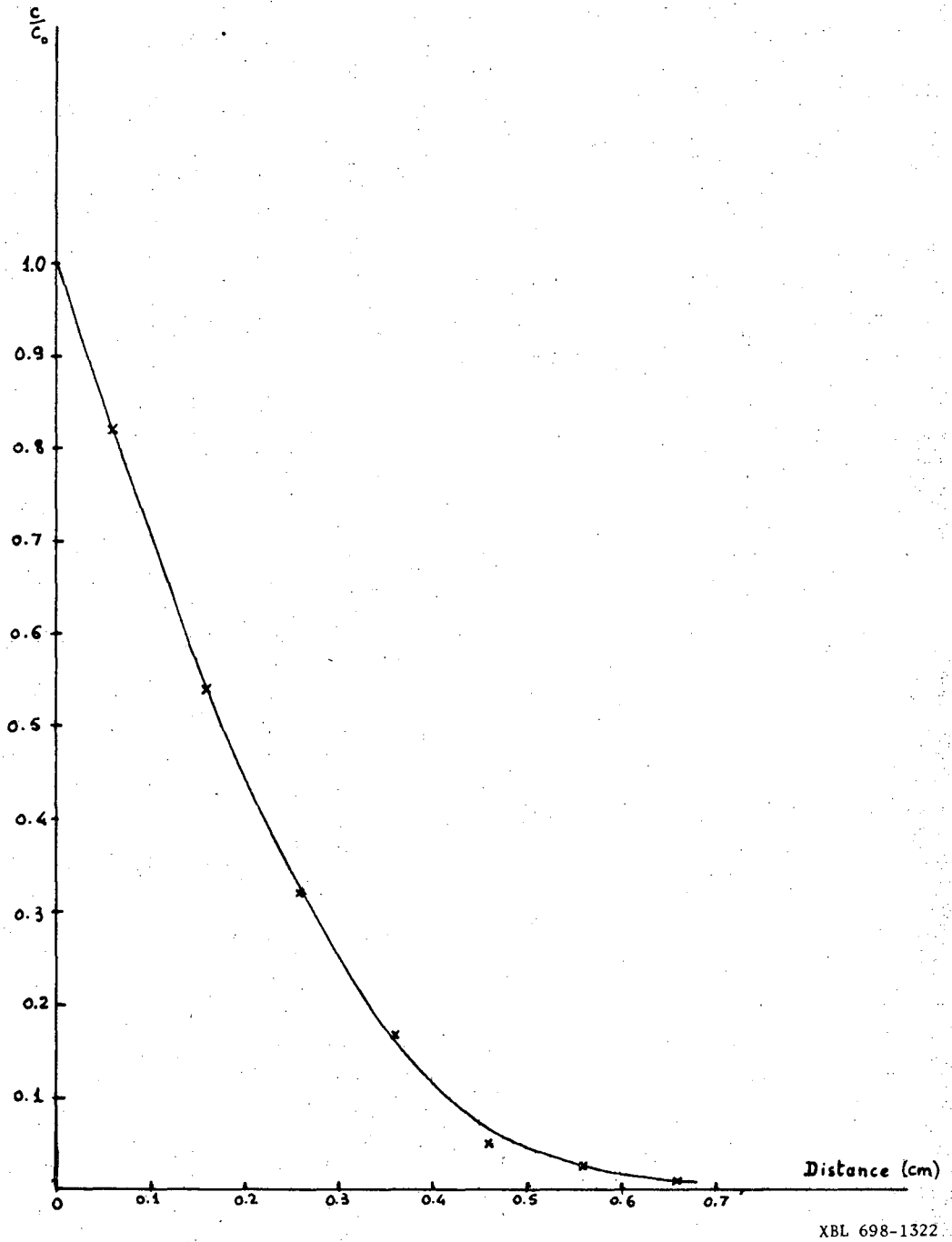
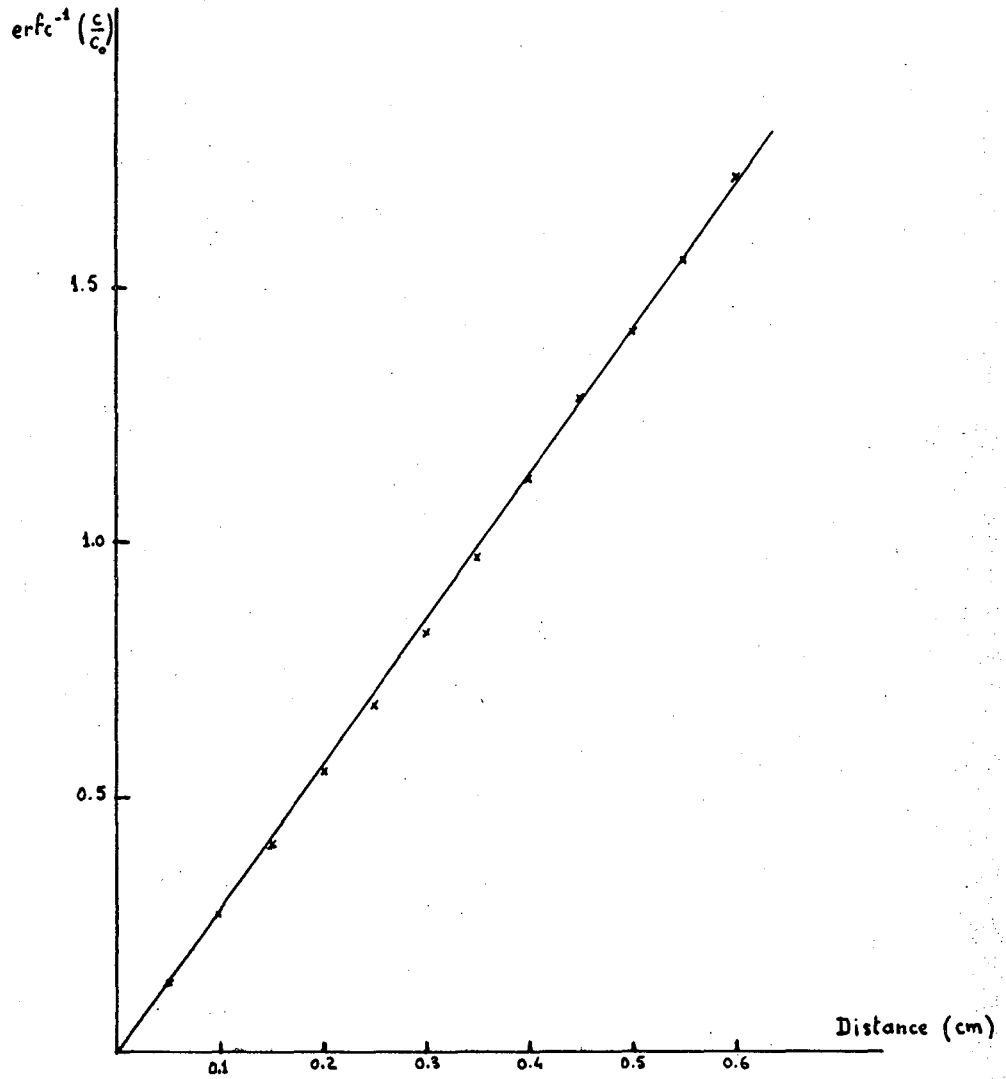
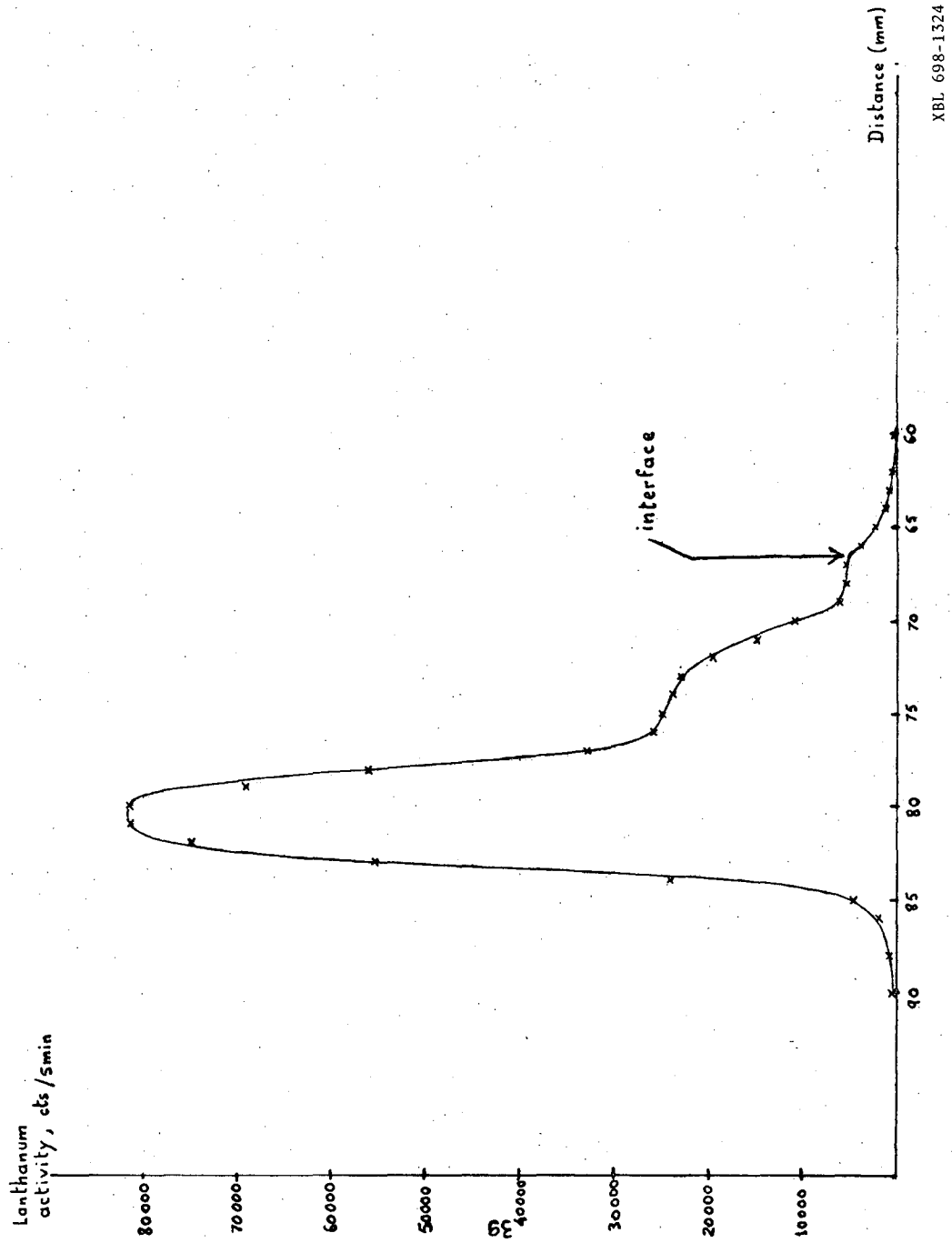


Fig. 16 Penetration curve - Run no. 3. The  $x = 0$  position on this plot is taken as the  $x = 54.4$  position on Fig. 12.



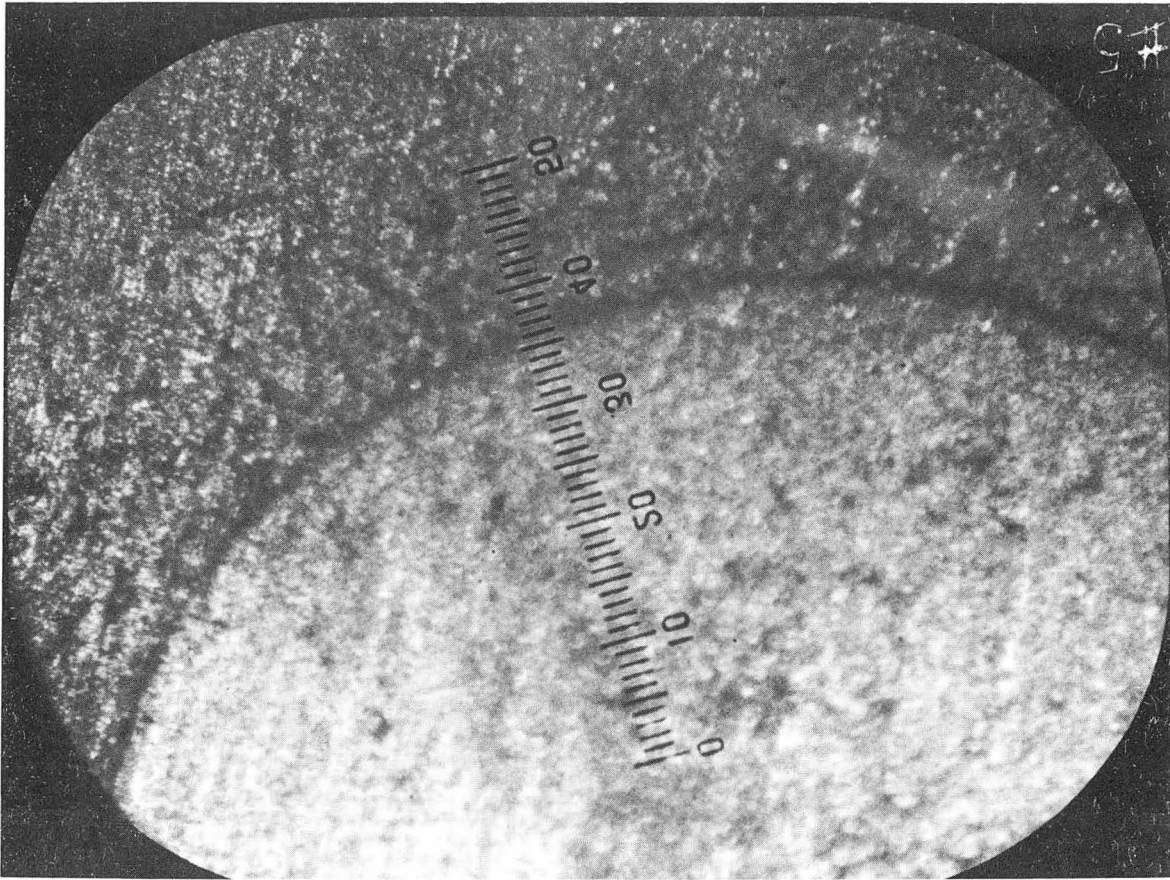
XBL 698-1323

Fig. 17 Determination of the diffusion coefficient -  
Run no. 3 - (Points from curve of Fig. 16).



XBL 698-1324

Fig. 18 Lanthanum concentration profile after diffusion - Run no. 5.



XBB 698-5520

Fig. 19 Lanthanum-uranium interface - Run no. 5  
( $\times 50$  - Lanthanum on top).



XBB 698-5515

Fig. 20 Lanthanum-uranium interface - Run no. 5  
( $\times 8.5$  - Lanthanum on top).

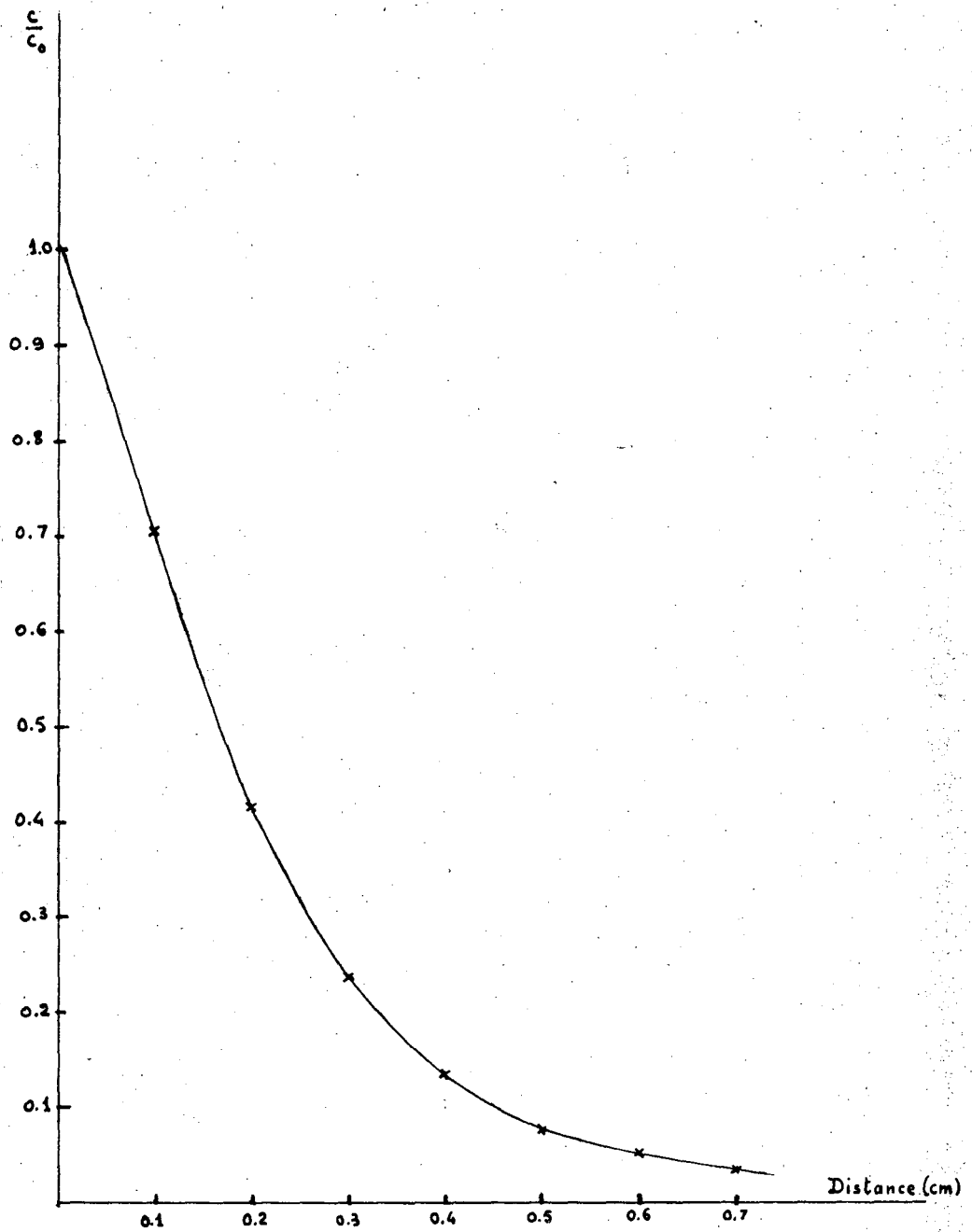
tantalum crucible. The plateau between 72 and 76 mm in Fig. 18 is due to a bubble in the lanthanum, which did not melt to form a continuous liquid. The ratio of the lanthanum concentration  $C$  to the lanthanum concentration  $C_0$  at the interface is plotted versus the distance  $x$  from the interface in Fig. 21, and the inverse complementary error function of  $\frac{C}{C_0}$  is plotted versus  $x$  in Fig. 22. Except for the last points, which scatter because of poor counting statistics, the experimental points were located on a straight line. However, this straight line did not pass exactly through the origin. Its slope gave a diffusion coefficient at  $1210^\circ\text{C}$  of  $5 \times 10^{-7} \text{ cm}^2 \text{ sec}^{-1}$ , which is very close to the value obtained in Run #3 with the tantalum crucible.

#### D. Conclusion

The only conclusion that could be drawn from this study is that the diffusion coefficient of lanthanum in molten uranium at  $1200^\circ\text{C}$  is very low, of the order of  $4 \times 10^{-7} \text{ cm}^2 \text{ sec}^{-1}$ . This is at least two orders of magnitude lower than most diffusion coefficients in liquid metals.<sup>2</sup>

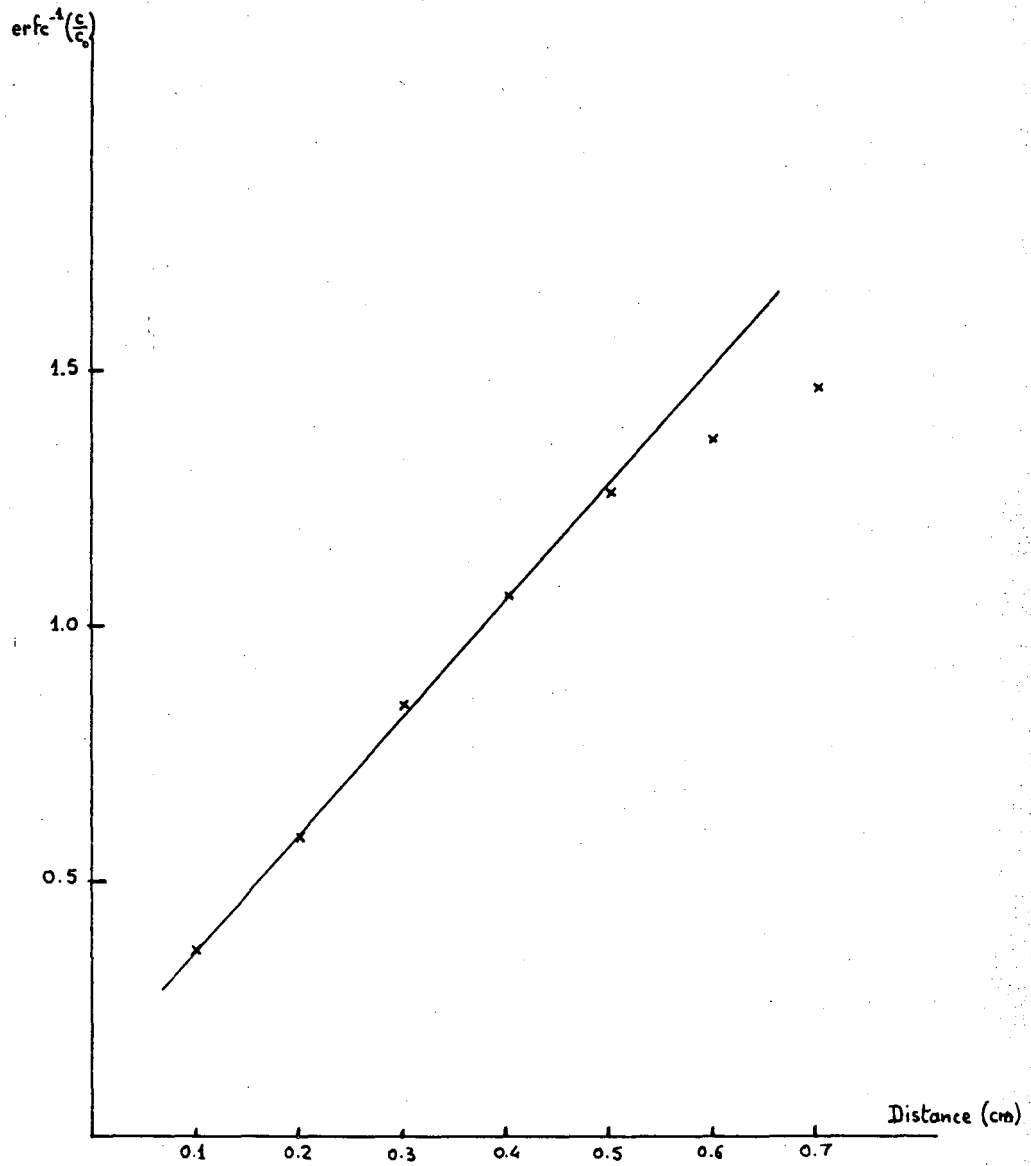
This low value of the diffusion coefficient could be explained by assuming that lanthanum diffuses through molten uranium not as a single atom, but as a complex formed by a lanthanum atom surrounded by a certain number of uranium atoms. Such complexes as  $\text{UCd}_{12}$  and  $\text{UZn}_{12}$  have already been discovered and the large size of the resulting complex considerably decreases the diffusion coefficient. However, a complex like  $\text{La}_n\text{U}_m$  has not yet been reported.

The very low diffusion coefficient of lanthanum in molten uranium could also be due to the presence of bubbles in the uranium. Those bubbles could be detected in all the experiments performed, despite all



XBL 698-1325

Fig. 21 Penetration curve - Run no. 5. The  $x = 0$  position on this plot is taken as the  $x = 67$  position on Fig. 18.



XBL 698-1326

Fig. 22 Determination of the diffusion coefficient - Run no. 5 - (Points from curve of Fig. 21).



efforts to avoid them. In a test run, four uranium rods were inserted each in a beryllia crucible, and the four samples were loaded into the vacuum resistance furnace shown in Fig. 2. After evacuating the furnace to  $10^{-6}$  torr and outgassing at  $1000^{\circ}\text{C}$  for 15 hours, the temperature was raised to  $1300^{\circ}\text{C}$  for 3 hours. The pressure during melting time never exceeded  $4 \times 10^{-6}$  torr. After melting, the four uranium surfaces were higher than expected by a distance varying from 2.8 to 4.5 cm, indicating extensive bubble formation during melting. The origin of these bubbles was probably dissolved gas in the uranium rods, which had not been prepared under high enough vacuum. The small bubbles formed anywhere in the uranium rod move upwards and join other bubbles. When the resulting bubble is large enough to contact the crucible wall, it is held there by surface tension forces rather than rising to the surface. Unfortunately, the bubbles tend to be trapped near the lanthanum-uranium interface. Furthermore, many small bubbles could be observed with a microscope in the uranium rod.

Those bubbles could be prevented by using crucibles with a larger inner diameter to permit unobstructed rise to the surface by decreasing the chance of a bubble coming in contact with the wall. Another method, which might be used concurrently, would be to vibrate the sample for a few minutes after melting (using the driving mechanism of an ultrasonic cleaner for example), so that all the bubbles could be released to the metal surface. However, it would be necessary to correct for the corresponding mixing which occurred during this period. Obtaining an exact value for the diffusion coefficient of lanthanum in molten uranium would require eliminating bubbles, whose effect on the measured diffusivities

could not be accurately assessed.

The good contact and general cleanliness of the lanthanum-uranium interfaces observed in the photomicrographs and the reasonable agreement of the solubility inferred from the activity measurements at various points in the rod of run #3 suggest that the equilibrium solubility is generated at the interface to drive the diffusion process.

The solubility of lanthanum in uranium ( $\sim 0.02$  atom fraction) is at least four orders of magnitude larger than the oxygen content of the uranium ( $\sim 25 \text{ ppm}^8$ ) so that complete conversion of the diffusing lanthanum to lanthana is unlikely. Since the crucibles were sealed under vacuum ( $10^{-5}$  torr) by electron beam welding, little contamination is expected from the small void volume remaining in the crucibles.

Tantalum and beryllia were satisfactory crucible materials. Both satisfactorily contained molten uranium at  $1300^\circ\text{C}$  for 3 hours and the lanthanum-uranium combination at  $1200^\circ\text{C}$  for 24 hours.

ACKNOWLEDGEMENTS

The author wishes to express his gratitude to Dr. Donald R. Olander for his constant assistance in both practical conduct and writing of this study. Appreciation is extended to Fran Silva whose help in welding the crucibles was invaluable.

This work was supported by the United States Atomic Energy Commission.

LIST OF NOMENCLATURE

- D diffusion coefficient of lanthanum in molten uranium,  $\text{cm}^2\text{sec}^{-1}$
- x distance along the uranium rod from bottom (part I) or from the interface (part II), cm
- $a_{\text{La}}^i(x)$  initial lanthanum concentration profile, counts/5 min.
- $a_{\text{La}}^o(x)$  lanthanum concentration profile after diffusion, corrected for decay, counts/5 min.
- $l$  length of the total uranium rod (irradiated + unirradiated), cm
- $\theta$  diffusion time, sec
- t time after diffusion experiment, sec
- $a_{\text{La}}$  lanthanum activity at time t, counts/5 min.
- $a_{\text{La}}^o$  lanthanum activity immediately after diffusion experiment, counts/5 min.
- $\lambda_{\text{La}}$  decay constant of lanthanum,  $\text{sec}^{-1}$
- $\lambda_{\text{Ba}}$  decay constant of barium,  $\text{sec}^{-1}$
- C lanthanum concentration at position x, counts/5min.
- $C_o$  lanthanum concentration at the interface, counts/5 min.

REFERENCES

1. D. R. Olander and A. D. Pasternak, Symposium on Nuclear Fuel Reprocessing, Ames Laboratory, August 1969, UCRL 19003 (1969).
2. A. D. Pasternak and D. R. Olander, AICHE Journal, 13, 1052 (1967).
3. T. Smith, Journal of the Electrochemical Society, 106, 1046 (1959).
4. K. Niwa, M. Shimoji, S. Kado, Y. Watanabe, and T. Yokokawa, Transactions AIME, 209, 96 (1957).
5. D. A. Morgan and J. A. Kitchener, Transactions Faraday Society, 50, 51 (1954).
6. Carslaw and Jaeger, Conduction of Heat in Solids, Oxford, London (1959).
7. J. F. Haefling and A.H. Daane, Transactions of the Metallurgical Society of AIME, 215, 336 (1959).
8. J. S. Finucane, UCRL-16988.

LEGAL NOTICE

*This report was prepared as an account of Government sponsored work. Neither the United States, nor the Commission, nor any person acting on behalf of the Commission:*

- A. Makes any warranty or representation, expressed or implied, with respect to the accuracy, completeness, or usefulness of the information contained in this report, or that the use of any information, apparatus, method, or process disclosed in this report may not infringe privately owned rights; or*
- B. Assumes any liabilities with respect to the use of, or for damages resulting from the use of any information, apparatus, method, or process disclosed in this report.*

*As used in the above, "person acting on behalf of the Commission" includes any employee or contractor of the Commission, or employee of such contractor, to the extent that such employee or contractor of the Commission, or employee of such contractor prepares, disseminates, or provides access to, any information pursuant to his employment or contract with the Commission, or his employment with such contractor.*

TECHNICAL INFORMATION DIVISION  
LAWRENCE RADIATION LABORATORY  
UNIVERSITY OF CALIFORNIA  
BERKELEY, CALIFORNIA 94720